Inorganic Chemistry
Cite This: Inorg. Chem. 2019, 58, 11614−11621
Article
pubs.acs.org/IC

# Synthesis and Investigation of Linker-Free BODIPY−Gly Conjugates Substituted at the Boron Atom

Maodie Wang,[†,‡] Guanyu Zhang,[†,‡] Petia Bobadova-Parvanova,[§] Ashley N. Merriweather,[†] Lilian Odom,[§] David Barbosa,[§] Frank R. Fronczek,[†] Kevin M. Smith,[†] and M. Graça H. Vicente*[,†]

[†]Department of Chemistry, Louisiana State University, Baton Rouge, Louisiana 70803, United States
[§]Department of Chemistry, Rockhurst University, Kansas City, Missouri 64110, United States

Supporting Information

**ABSTRACT:** An efficient synthesis of boron-functionalized cyclic BODIPY−Gly conjugates, using commercially available *N*-protected glycine amino acids and a $BF_2$−BODIPY moiety as starting materials, is reported. The existence of two conformers (up and down) is revealed through comprehensive DFT calculations and $^1$H and $^{11}$B NMR analyses. The experimental and computational results indicate that all BODIPYs are stable in aqueous solutions at neutral pH and that Fmoc-BODIPY (**4**) is more stable than Ac-BODIPY (**6**) in the presence of trifluoroacetic acid (TFA). In part due to their enhanced rigidity, all BODIPY−Gly conjugates display increased fluorescence quantum yields ($0.6 < \Phi < 0.9$) relative to the corresponding $BF_2$−BODIPY, making them excellent candidates for fluorescence imaging applications.

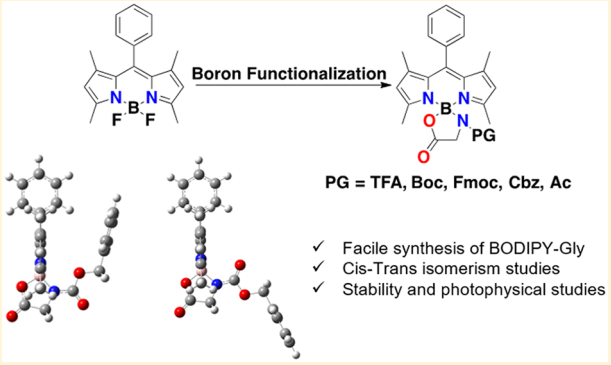


## INTRODUCTION

Boron dipyrromethene (BODIPY) dyes[1−3] are a class of boron-coordinated organic heterocycles with excellent photophysical properties, including large molar extinction coefficients, sharp absorptions and emissions in the visible region of the optical spectrum, and high fluorescence quantum yields. The last two decades have witnessed various applications of BODIPY dyes, including living cell bioimaging,[4] photodynamic therapy,[5] and fluorescence sensing[6] and their use in dye-sensitized solar cells.[7] The properties of BODIPY dyes can be fine-tuned via functionalization at the various peripheral positions,[8] for example allowing the preparation of BODIPYs with extended $\pi$-conjugated systems that absorb and emit in the near-IR region of the optical spectrum,[9−13] and/or of water-soluble BODIPYs.[14−16] In particular, functionalization at the boron position results in only slight changes in the absorption and/or emission wavelengths of BODIPY dyes, but can be used to increase the fluorescence quantum yields, Stokes shifts, aqueous solubility, stability, and the redox and aggregation properties of this type of dye.[12−17] Despite extensive studies of *CN*-BODIPYs,[18,19] *O*-, and *C*-BODIPYs (alkyl, aryl, ethynyl, and ethynylaryl),[20,21] the investigation of the corresponding *N*-BODIPYs has lagged far behind. Recently it was reported that starting from $BCl_2$−BODIPYs,[22,23] the corresponding *N*-BODIPYs[24,25] can be synthesized via substitution of the chlorines with various *N*-nucleophiles.

Molecular imaging based on the conjugation of fluorescent dyes with affinity ligands, such as peptides and antibodies, is an emerging modality in cancer diagnosis and therapy. Traditional conjugation methods require the introduction of reactive functionalities on the BODIPY core, for example an azide or ethynyl group for "click" reactions, or an isothiocyanato as an amino reacting group.[26] In 2016, the first linker-free BODIPY peptide conjugates were synthesized through palladium-catalyzed C($sp^2$-H) activation, allowing for direct conjugation with Trp-containing peptides.[27] More recently, Ackermann and co-workers reported the palladium-catalyzed C($sp^3$-H) activation for BODIPY peptide labeling, thus extending direct conjugation to Ala- and Phe-containing peptides.[28] Herein, we report, for the first time, a method for the synthesis of linker-free BODIPY-glycine derivatives via functionalization at the boron atom that can be extended to the conjugation of any $\alpha$-amino acid to a BODIPY. We investigated the effects of different protecting groups at the *N*-terminus of glycine on the reaction yields, spectroscopic properties, and stability of the resulting BODIPY conjugates under aqueous neutral or acidic conditions (TFA), using both experimental and computational methods. Our results show that the acid stability and fluorescence quantum yields of the BODIPY−Gly conjugates depend on the protecting group at the N-terminus of glycine.

## RESULTS AND DISCUSSION

**Synthesis.** An electron-withdrawing group on nitrogen is necessary for the synthesis of stable *N*($sp^3$)-BODIPYs, since this decreases the charge on the boron atom.[24,25] In the

Received: May 22, 2019
Published: August 20, 2019






DOI: 10.1021/acs.inorgchem.9b01474
Inorg. Chem. 2019, 58, 11614−11621

present study, five commercially available glycine derivatives, with different carbonyl-based protecting groups on the *N*-terminus, were used to functionalize BODIPY **1** at the boron position in a two-step one-pot reaction under mild conditions, as shown in Scheme 1. BODIPYs **2**–**6** were synthesized from

**Scheme 1. Synthesis of BODIPY–Gly Derivatives 2–6**

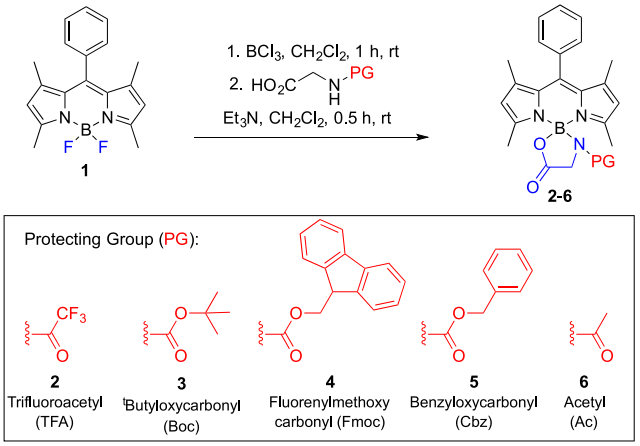


*in situ* generated $BCl_2$–BODIPY from the reaction of **1** with boron trichloride, followed by reaction of *N*-protected Gly, in 25–62% isolated yields. The cyclic *N*,*O*-bidentate BODIPYs **2**–**6** were the major products obtained when 1–2 equiv of N-protected Gly were used in the presence of triethylamine, in dichloromethane solution at room temperature. Side products identified in this reaction were the corresponding BODIPYs bearing one Gly and one fluorine on the boron atom, and the bis(Gly)–BODIPY derivatives. The difference in the reaction yields obtained when different glycine *N*-protecting groups were used suggests that BODIPYs **2**–**6** might display different stability and/or solubility in organic solvents. Therefore, we further investigated the structural and dynamic features of BODIPYs **2**–**6** using both spectroscopic and computational analyses.

**Cis–Trans Isomerism.** BODIPYs **2**–**6** were all characterized by $^1$H, $^{11}$B, and $^{13}$C NMR spectroscopies in $CDCl_3$ or $CD_2Cl_2$ solution (see Figures S1–S16 of the Supporting Information). Surprisingly, two sets of peaks were observed in the $^1$H NMR spectra of BODIPYs **2** (TFA), **4** (Fmoc), and **5** (Cbz). In particular, the protons at the 2,6-positions of BODIPY **4** split into two singlets at 6.10 and 5.97 ppm in the integration ratio of 1:0.27 (see Figure 1c). The protons at the $\alpha$-position of the glycine residue and the methyl groups at the 1,3,5,7-positions of BODIPY **4** are all similarly split (see Figure S8 of the Supporting Information). This clearly suggests the existence of two BODIPY conformers at room temperature in $CDCl_3$. Trans- and cis-isomerism is common in amide bond-containing molecules due to p–$\pi$ conjugation and the resulting rotational barrier for the amide bond.[29,30] Indeed, B3LYP/6-31+G(d,p)-optimization for BODIPYs **2**–**6** demonstrated the existence of two possible conformers (up and down, as shown in Figure 1a,d). The calculated properties of these conformers are shown in Table 1. The differences in the energies and Gibbs-free energies of the two conformers were negligible at the B3LYP/6-31+G(d,p) level. Therefore, these were calculated at the $\omega$B97X-D/6-31+G(d,p) level to include empirical dispersion. As seen in Table 1, the differences in the Gibbs free

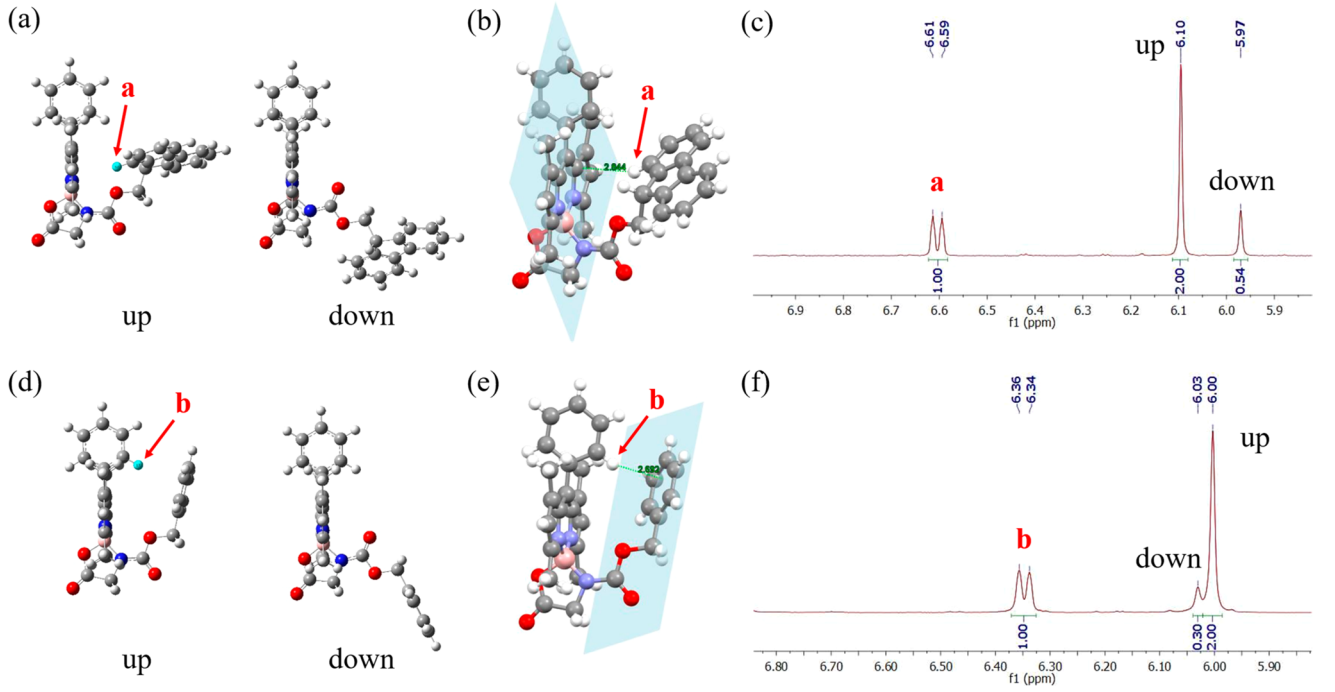


**Figure 1.** Unusual cases of BODIPYs **4** and **5**: (a) B3LYP/6-31+G(d,p)-optimized structures of the up- and down-conformers of BODIPY **4** in chloroform. The highly shielded aromatic proton is labeled with "a". (b) X-ray crystal structure of BODIPY **4**. (c) Aromatic region of the $^1$H NMR spectrum of BODIPY **4** in $CDCl_3$. Protons at the 2,6-position of BODIPY **4** are split in a 1:0.27 ratio. The proton "a" at 6.60 ppm belongs to the up-conformer. (d) B3LYP/6-31+G(d,p)-optimized structure of the up- and down-conformers of BODIPY **5**. The highly shielded aromatic proton is labeled with "b". (e) X-ray crystal structure of BODIPY **5**. (f) Aromatic region of the $^1$H NMR spectrum of BODIPY 5 in $CD_2Cl_2$. Protons at the 2,6-position of BODIPY 5 are split in 1:0.15 ratio. Proton "b" at 6.35 ppm belongs to the up-conformer.



DOI: 10.1021/acs.inorgchem.9b01474
*Inorg. Chem.* 2019, 58, 11614–11621

**Table 1. Molecular Properties for the Series of BODIPYs Studied**[a]

| BODIPY | conformer | $\Delta G_{up-down}$ (kcal/mol) | dipole moment (D) | $r_{BN}$ (Å) | $\Delta E_{rotation}$ (kcal/mol) | $^{11}B_{calc}$ (ppm) | $^{11}B_{exp}$ (ppm) | $q_B$ (au) | $V_B$ (au) |
|---|---|---|---|---|---|---|---|---|---|
| **2** (TFA) | up | | 9.73 | 1.559 | 17.9 | 0.79 | 1.83 | 1.155 | −11.3567 |
| | down | 0.69 | 6.99 | 1.547 | | 1.84 | 2.54 | 1.159 | −11.3668 |
| **3** (Boc) | up | | 11.07 | 1.523 | 16.6 | 0.71 | 1.97 | 1.157 | −11.3783 |
| | down | 2.94 | 7.14 | 1.522 | | 1.55 | | 1.158 | −11.3853 |
| **4** (Fmoc) | up | | 10.44 | 1.531 | 23.0 | 0.73 | 2.11 | 1.158 | −11.3713 |
| | down | 8.20 | 6.90 | 1.525 | | 1.77 | | 1.159 | −11.3814 |
| **5** (Cbz) | up | | 10.69 | 1.529 | 20.3 | 0.73 | 1.98 | 1.157 | −11.3744 |
| | down | 5.54 | 6.58 | 1.525 | | 1.38 | | 1.158 | −11.3828 |
| **6** (Ac) | up | | 11.79 | 1.530 | 18.8 | 1.15 | 2.18 | 1.159 | −11.3701 |
| | down | 3.76 | 5.10 | 1.529 | | 1.59 | | 1.159 | −11.3820 |

[a]Gibbs free energy difference between the two conformers, $\Delta G_{up-down}$, dipole moment, B−N bond length between B and glycine N ($r_{BN}$); energy barrier of rotation, $\Delta E_{rotation}$, calculated and experimentally determined $^{11}B$ chemical shifts, NPA atomic charges ($q_B$), and molecular electrostatic potential ($V_B$) at the boron atom. All parameters are calculated in chloroform. Gibbs free energies, dipole moments, atomic charges, molecular electrostatic potential, and bond lengths are calculated at the ωB97X-D/6-31+G(d,p) level. NMR parameters are calculated at the B3LYP/6-31+G(d,p) level. $BF_3{\cdot}OEt_2$ is used as the reference for the $^{11}B$ NMR calculations.

energies are small but a trend exists, with the up-conformer consistently more stable than the corresponding down-conformer, especially for the BODIPYs with aromatic protecting groups (**4** and **5**). On the other hand, the BODIPY B−N(Gly) bond lengths are similar for both the up- and down-conformers, with BODIPY **2** having the weakest B−N(Gly) bond, and the largest difference between the bond lengths of the conformers. Other bond lengths are given in Table S1 of the Supporting Information. No significant differences were observed between the other bond lengths of the two conformers for the different BODIPYs **2**−**6**. According to our calculations, the major difference that exists between the two conformers is their polarity—all up-conformers have significantly higher dipole moments compared with the down-conformers (Table 1). This is consistent with the two carbonyl groups pointing in the same direction in the case of the up-conformers.

For all compounds, the up- and down-conformers interconvert through rotation around the glycine C−N bond. The calculated rotational barriers (Table 1) are similar in all cases, with those for BODIPYs with aromatic protecting groups (**4** and **5**) slightly higher than for the other BODIPYs (**2**, **3** and **6**). All rotational barriers are around 20 kcal/mol, indicating that both up- and down-conformers most likely exist in chloroform solution at room temperature.

The B3LYP/6-31+G(d,p)-simulated $^1H$ NMR spectra are consistent with the observed two sets of proton peaks and indicate that they are due to the coexistence of both the up- and down-conformers. For BODIPY **4** (Fmoc), the doublet at 6.60 ppm corresponding to proton "a" and the singlet at 6.10 ppm corresponding to the 2,6-protons are, as expected, in a 1:2 ratio (Figure 1c). The peak denoted with "a" corresponds to a highly shielded aromatic proton in the Fmoc group of the up-conformer of BODIPY **4**. The observed shielding is due to the anisotropic effect of the BODIPY core. It should be noted that the Fmoc group is tilted with one phenyl ring toward the BODIPY unit and the other one away from it (see Figure S17 of the Supporting Information). Therefore, there is only one proton "a" in the up-conformer that experiences the ring-current effect. In the down-conformer, the Fmoc is too far away from the BODIPY core for an effect to be observed.

Peaks corresponding to the two conformers are also observed in the $^1H$ NMR spectrum for BODIPY **5**. In this case the *meso*-phenyl hydrogen atom denoted with "b" in Figure 1d is shielded by the protecting group phenyl, resulting in a peak at 6.35 ppm (Figure 1f). In the down-conformer, the protecting group phenyl is too far away from the BODIPY core; therefore, no effect is observed.

The observed ratios of conformers for BODIPYs **4** and **5** suggest that the up-conformer dominates in chloroform solution. This is consistent with the calculated lower energies for the up-conformers, especially in the case of BODIPYs **4** and **5** (Table 1). For BODIPYs **2** (TFA), **3** (Boc), and **6** (Ac) no shielding effects are observed in the $^1H$ NMR spectra due to the lack of an aromatic moiety in their protecting group. The computationally modeled spectra in the case of BODIPYs **3** and **6** show almost identical chemical shifts for the two up- and down-conformers, and as a consequence, only one set of $^1H$ NMR signals is observed experimentally in these cases.

Table 1 also lists the calculated and experimentally observed $^{11}B$ chemical shifts for BODIPYs **2**−**6** in $CDCl_3$. The simulated NMR spectra show two $^{11}B$ NMR peaks for all BODIPYs, corresponding to the up- and down-conformers. However, the difference in the chemical shift is small, and as a result most BODIPYs show a single peak experimentally at around 2 ppm. BODIPY **2** is the exception, showing two peaks in its $^{11}B$ NMR spectrum (see Figure S3 of the Supporting Information). This is probably due to the larger difference between the up- and down-conformer chemical shifts, as suggested by the calculated values (Table 1).

The calculated values also indicate that the up-conformers have a slightly smaller chemical shift compared with the down-conformers. This is consistent with the observed atomic charge on the boron atom ($q_B$, Table 1), as we have previously reported,[17,18,31] and with the molecular electrostatic potentials at the boron atom ($V_B$, Table 1). Since the differences between the calculated boron charges are small, the trend becomes apparent when comparing the values of $V_B$. As reported previously,[32,33] the molecular electrostatic potentials are more sensitive to the electronic distribution than the atomic charges, and also do not suffer from additional approximations. The results indicate that all down-conformers have consistently deeper potentials corresponding to greater deshielding and, consequently, higher NMR shifts.

**Crystal Structures.** Suitable crystals of BODIPYs **2** and **4** for X-ray analysis were obtained by slow evaporation of dichloromethane and hexane, while BODIPY **5** crystals were grown by slow evaporation of dichloromethane. The results are



DOI: 10.1021/acs.inorgchem.9b01474
Inorg. Chem. 2019, 58, 11614−11621

shown in Figure 2. For all three structures, both the five- and six-membered rings at the spiro boron atom are nearly planar.

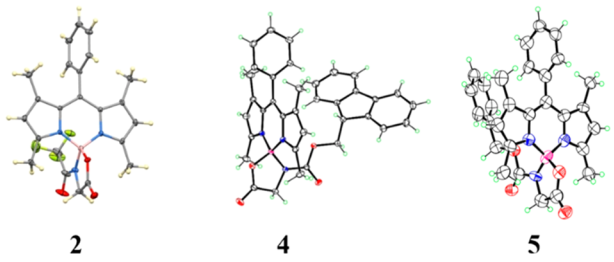


**Figure 2.** Crystal structures of BODIPYs **2**, **4**, and **5** with 50% ellipsoids.

For the six-membered $BN_2C_3$ ring, mean deviations are 0.005 Å for **2**, 0.021 Å for **4**, and 0.018 Å for **5**. For the five-membered $BNOC_2$ ring, deviations are 0.014 Å for **2**, 0.007 Å for **4**, and 0.012 Å for **5**. Also, in all three structures, the two spiro rings are nearly orthogonal, forming dihedral angles of 88.9° for **2**, 89.9° for **4**, and 89.4° for **5**. B−N distances in these rings are in the range 1.5309(18)−1.5654(18) Å for **2**, 1.5426(9)−1.5442(9) Å for **4**, and 1.50(2)−1.574(18) Å for **5**. The B−O distances are 1.4896(17) Å for **2**, 1.4936(9) Å for **4**, and 1.498(18) Å for **5**. The N−B−N bite angle of the 6-membered ring is 107.66(10)° for **2**, 106.93(5)° for **4**, and 105.7(12)° for **5**. The O−B−N bite angle in the 5-membered ring is 100.64(10)° for **2**, 100.98(5)° for **4**, and 101.4(12)° for **5**. All these values are in good agreement with those found in a previously reported chiral BODIPY,[34] which has dihedral angle of 89.2° between the two spiro rings, B−N distances 1.524(3) − 1.549(3) Å, B−O distance 1.492(3) Å, and bite angles of 106.86(15) and 100.89(14)°.

**Stability Studies.** We further investigated the stability of BODIPYs **4**, bearing a Fmoc protecting group, and **6** bearing an acetyl group, by $^1$H and $^{11}$B NMR spectroscopy in $CDCl_3$ upon addition of 1 equiv of trifluoroacetic acid (TFA).[17] Under these conditions, the potential formation of BODIPYs **7** and **8**, respectively (see Scheme S1 of the Supporting Information) was investigated overtime. In fact, we observed that immediately after protonation some of the BODIPY protons showed a slight downfield shift. For example, the 2,6-protons of BODIPY **6** immediately shifted from 6.05 to 6.11 ppm. This is due to the protonation of the Gly residue, which likely occurs on the carbonyl oxygen atom of the protecting group. One hour after TFA addition to BODIPY **6**, a new set of 2,6-protons appeared at 6.00 ppm and the intensity of this new signal increased with time while that of the 6.11 ppm signal decreased. Similarly, in the aliphatic region, new signals appeared at 1.42 and 2.40 ppm that increased with time, while the signals for the 1,3,5,7-methyls of BODIPY **6** decreased with time. Moreover, in the $^{11}$B NMR spectrum, a new signal appeared upfield at 0.2 ppm, 4 h after TFA addition to BODIPY **6**. These results suggest the formation of a new BODIPY upon TFA addition, likely bearing a trifluoroacetate group in addition to a Gly residue on the boron atom (see BODIPY **8** in Scheme S1 of the Supporting Information). Indeed, BODIPY **8** was identified by $^1$H and $^{11}$B NMR and MS-ESI spectroscopies (see Figures S18, S19, and S22 of the Supporting Information). In the $^1$H NMR spectrum a new doublet was observed at 4.11 ppm corresponding to the $\alpha$-protons of the glycine residue of BODIPY **8**, split by the adjacent N−H proton which appears as a triplet at 6.47 ppm. We hypothesize that upon addition of TFA to BODIPY **6**, the B−N(Gly) bond weakens due to protonation of the glycine residue, and this is followed by trifluoroacetate attack on the boron atom with formation of BODIPY **8**.

Under the same acidic conditions, BODIPY **4** bearing a Fmoc protecting group was more stable than **6**, with new peaks appearing in the $^1$H and $^{11}$B NMR spectra only 9 h after addition of TFA (see Figures S20, S21, and S23 of the Supporting Information) likely due to the formation of BODIPY **7**. The enhanced stability observed for BODIPY **4** relatively to **6** is possibly due to enhanced stabilizing intramolecular interactions and/or decreased boron accessibility due to the larger Fmoc protecting group. Interestingly, the ratio of the up- and down-conformers of **4** also changed upon addition of TFA, which might be a result of the different stabilities of the two conformers, as suggested by the different B−N(Gly) bond lengths. These results indicate that different protecting groups on the glycine residue result in BODIPY−Gly derivatives of different stability under acidic conditions,

**Table 2. Experimental and Calculated Spectroscopic Properties of BODIPYs in Acetonitrile at Room Temperature**[a]

| | | $\Delta E_{S0\sim S1}$ (eV) | $\lambda_{abs}$ (nm) | | oscillator strength | log $\varepsilon$ ($M^{-1}cm^{-1}$) | $\lambda_{em}$ (nm) | $\Phi_f$[b] | Stokes shift ($cm^{-1}$) | | |
|---|---|---|---|---|---|---|---|---|---|---|---|
| BODIPY | conformer | calcd | calcd | expt | calcd | expt | expt | expt | expt | $\nu_{out\text{-}of\text{-}plane}$ ($cm^{-1}$) | $k_{out\text{-}of\text{-}plane}$ (mDyne/Å) |
| **1** | – | 2.87 | 431 | 498 | 0.617 | 4.84 | 510 | 0.50 | 12 | 469 | 1.04 |
| **2** (TFA) | up | 2.86 | 433 | 503 | 0.526 | 4.75 | 514 | 0.87 | 11 | 703 | 2.27 |
| | down | 2.86 | 433 | | 0.537 | | | | | 709 | 2.41 |
| **3** (Boc) | up | 2.85 | 436 | 503 | 0.508 | 4.67 | 513 | 0.90 | 10 | 704 | 2.40 |
| | down | 2.86 | 434 | | 0.526 | | | | | 703 | 2.41 |
| **4** (Fmoc) | up | 2.83 | 438 | 503 | 0.448 | 4.73 | 515 | 0.62 | 12 | 704 | 2.40 |
| | down | 2.86 | 434 | | 0.518 | | | | | 705 | 2.48 |
| **5** (Cbz) | up | 2.84 | 436 | 503 | 0.498 | 4.85 | 514 | 0.76 | 11 | 703 | 2.41 |
| | down | 2.86 | 434 | | 0.526 | | | | | 703 | 2.26 |
| **6** (Ac) | up | 2.86 | 433 | 502 | 0.528 | 4.76 | 513 | 0.80 | 11 | 713 | 2.16 |
| | down | 2.86 | 433 | | 0.544 | | | | | 710 | 2.08 |

[a]All parameters are calculated at M06-2X/6-31+G(d,p) level in acetonitrile. The leading transition is HOMO → LUMO for all calculated molecules. The last two columns represent the unscaled frequency of the boron out-of-plane vibrational mode $\nu_{out\text{-}of\text{-}plane}$ and the respective force constant, $k_{out\text{-}of\text{-}plane}$. [b]Fluorescein (0.91 in 0.1 M NaOH) was used as the standard.



DOI: 10.1021/acs.inorgchem.9b01474
Inorg. Chem. 2019, 58, 11614−11621

likely due to a change in the p-$\pi$ conjugation upon protonation of the Gly residue.[29,30]

The aqueous stability of 10 $\mu$M solutions of BODIPYs **2**–**6** was also investigated in 1:9 or 1:1 DMSO/phosphate buffered saline (PBS) at pH 7.4, to ensure solubility of the BODIPYs in aqueous media. As can be seen from the absorption and emission spectra (see Figures S24–S35 of the Supporting Information), the characteristic BODIPY bands show no changes in the maximum absorption/emission wavelengths nor intensities for up to 5 days, suggesting that all BODIPYs are stable in aqueous solution at neutral pH.

**Spectroscopic Properties.** The spectroscopic properties of BODIPYs **1**–**6** were measured in acetonitrile (see Figures S36 and S37 of the Supporting Information) and the results are summarized in Table 2. All glycine functionalized BODIPYs **2**–**6** show very similar absorption and fluorescence profiles compared with starting BODIPY **1**. The maximum absorption wavelengths are very similar, slightly red-shifted (by 4–5 nm) compared with **1**. This is consistent with the performed calculations (Table 2). The calculations performed at the M06-2X/6-31+G(d,p) level predict very similar values for all BODIPYs **2**–**6** and a small red-shift (2–7 nm) compared with BODIPY **1**. The same trend is observed for the maximum emission wavelengths, which are slightly red-shifted by 3–5 nm compared with **1**. Most importantly, all BODIPY–Gly conjugates **2**–**6** were found to have significantly higher fluorescence quantum yields ($0.6 < \Phi < 0.9$) than $BF_2$–BODIPY **1** ($\Phi = 0.5$). This might be a result of increased rigidity around the spiro boron atom of the BODIPY–Gly derivatives, as suggested by the calculated values of the frequency of the boron out-of-plane vibrational mode and the corresponding force constant (Table 2). Upon glycine substitution with formation of the *N*,*O*-bidentate 5-member ring BODIPYs, both the values for the frequency of the boron out-of-plane vibration and the force constant significantly increase, and therefore, it becomes harder for the boron atom to move out of the plane of the BODIPY core, resulting in less energy loss to nonradiative decay.

Figure 3 represents the frontier orbitals of the up- and down-conformers of BODIPY **6**. As can be observed, both HOMO and LUMO are localized on the BODIPY core with no contribution from glycine and its protecting group. A similar situation exists for all other synthesized BODIPYs (see Figure S38 of the Supporting Information). Therefore, the different protecting groups do not affect significantly the energies of the HOMO and LUMO. All up-conformers have consistently lower HOMO and LUMO energies than their respective down-analogs. However, the effect is very small. The performed TD-DFT calculations indicate that the HOMO → LUMO is the leading transition for all BODIPYs studied. Since both the forms and energies of these two orbitals are generally independent of the protecting group, it is not surprising that the absorptions and emissions observed for the BODIPY–Gly derivatives are similar among the entire series.

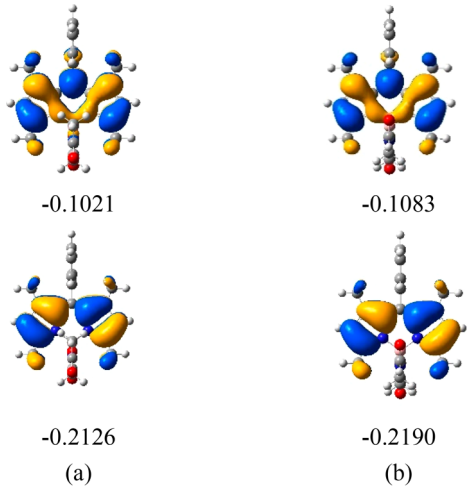


**Figure 3.** Frontier orbitals of (a) the up-conformer and (b) the down-conformer of BODIPY **6** (Ac). Orbital energies in au. The frontier orbitals of all conformers of all BODIPYs studied are given in the Supporting Information (Figure S38).

## CONCLUSIONS

The facile one-pot synthesis of BODIPY–Gly derivatives from a $BF_2$–BODIPY is demonstrated. These novel linker-free *N*,*O*-bidentate BODIPYs were prepared in moderate yields via nucleophilic substitution in the presence of boron trichloride, at room temperature. The resulting BODIPY–Gly derivatives were investigated computationally and experimentally. At room temperature in chloroform solution, the BODIPY–Gly derivatives exist as two conformers – up and down—depending on the orientation of the glycine protecting group. The rotational barrier between the two conformers is around 20 kcal/mol. The up-conformer was found to be the most stable, particularly in the case of BODIPY–Gly bearing aromatic protecting groups (**4** and **5**), and to predominate in chloroform solution. The two conformers have similar B–N(Gly) bond lengths but distinct polarities, with the up-conformers displaying higher dipole moments than the down-conformers. In the presence of one equivalent of TFA, BODIPY–Gly **4** bearing a Fmoc protecting group was found to be more stable than **6** bearing an acetyl group, maybe due to enhanced intramolecular interactions and/or decreased boron accessibility in the case of **4**. On the other hand, all BODIPY–Gly derivatives were found to be stable in aqueous solution at neutral pH. The absorption and fluorescence emission spectra of the BODIPY–Gly derivatives show slight red-shifted bands relative to those of the $BF_2$–BODIPY. However, all BODIPY–Gly derivatives display increased fluorescence quantum yields as a result of increased rigidity around the spiro boron atom. Overall, our results show that linker-free BODIPY–Gly derivatives are easily prepared, and that the reaction yields, stability, polarity and fluorescence quantum yields of the products depend on the glycine protecting groups. The BODIPY–Gly bearing a Fmoc protecting group was isolated in the highest yield (62%) and showed enhanced stability under acidic conditions (TFA), while the BODIPY–Gly bearing a Boc protecting group displayed the highest fluorescence quantum yield ($\Phi = 0.9$).

## EXPERIMENTAL SECTION

**General Data.** All commercially available chemical reagents were purchased from VWR or Sigma-Aldrich and used without further purification. All product yields refer to isolated yields after column chromatography using Sorbent Technologies silica gel (60 Å, 230–400 mesh). The $^{1}H$, $^{13}C$, $^{11}B$ and $^{19}F$ NMR spectra were collected using a Bruker AV-400 or AV-500 spectrometer at 300 K in deuterated chloroform (7.26 ppm for $^{1}H$ and 77.0 ppm for $^{13}C$) or deuterated dichloromethane (5.30 ppm for $^{1}H$) by operating at 400 MHz for $^{1}H$ NMR, 126 MHz for $^{13}C$ NMR, 128 MHz for $^{11}B$ NMR,



DOI: 10.1021/acs.inorgchem.9b01474
Inorg. Chem. 2019, 58, 11614–11621

and 471 MHz for $^{19}F$ NMR. $BF_3{\cdot}OEt_2$ was used as the reference (0.00 ppm) for $^{11}B$ NMR spectra; $CFCl_3$ was used as the reference (0.00 ppm) for $^{19}F$ NMR spectra. High-resolution mass spectra were collected using an Agilent 6230-B ESI-TOF mass spectrometer in positive mode. All melting points were recorded using a MELTEMP electrothermal apparatus. UV−vis absorption spectra of ca. $10^{-5}$ M solutions of BODIPYs were recorded. Emission spectra ($\lambda_{ex}$ = 470 nm) of ca. $10^{-5}$ M solutions were recorded in quartz cells. Relative fluorescence quantum yields ($\Phi_f$) were calculated using fluorescein ($\Phi_f$ = 0.91 in 0.1 M NaOH) as the standard using the following equation:

$$\Phi_X = \Phi_{ST}(\mathrm{Grad}_X/\mathrm{Grad}_{ST})(\eta_X/\eta_{ST})^2$$

where $\Phi_X$ and $\Phi_{ST}$ are the quantum yields of the sample and standard, $\mathrm{Grad}_X$ and $\mathrm{Grad}_{ST}$ are the gradient from the plot of integrated fluorescence intensity vs absorbance, and $\eta$ is the refractive index of the solvent. BODIPY **1** was prepared as previously reported in the literature.[31,35−37]

**Computational Methods.** The geometries of all BODIPYs and complexes were optimized without symmetry constraints. The stationary points on the potential energy surface were confirmed with frequency calculations. The solvent effects were taken into account using the polarized continuum model (PCM).[38] All reported energies, geometry parameters, atomic charges, molecular electrostatic potentials, and dipole moments were calculated at the $\omega$B97X-D/6-31+G(d,p) level to include empirical dispersion.[39] The atomic charges were calculated using the NPA scheme.[40] The NMR chemical shifts were calculated using the gauge-independent atomic orbital (GIAO) method[41] at the B3LYP/6-31G(d,p) level,[42,43] which is shown to provide reliable NMR data.[44] The UV−vis absorption data were calculated using the TD-DFT method[45] and the M06-2X/6-31+G(d,p) level[46] as recommended in the literature.[47] All calculations were performed using the Gaussian 09 program package.[48]

**Crystallography.** Crystals of BODIPYs **2** and **4** were obtained by slow evaporation of dichloromethane and hexane, while those of **5** were grown by slow evaporation of dichloromethane. X-ray diffraction data for **2**, **4** hemihexane solvate, and **5** were measured at low temperature on a Bruker Kappa Apex-II DUO diffractometer with either MoK$\alpha$ or Cu K$\alpha$ radiation. Refinement was by full-matrix least-squares, treating nonhydrogen atoms anisotropically. H atoms were visible in difference maps, but were placed in idealized positions for refinement. Crystal data for **2**, $C_{23}H_{21}BF_3N_3O_3$, FW = 455.24, orthorhombic space group $P2_12_12_1$, $a$ = 7.9096(2), $b$ = 10.8412(3), $c$ = 25.8387(6) Å, $T$ = 90 K, $Z$ = 4. A total of 19 637 data were collected with Mo K$\alpha$ radiation to $\theta_{max}$ = 34.4°, $R$ = 0.040 for 8038 data with $I > 2\sigma(I)$ of 8504 unique data ($R_{int}$ = 0.019), 302 refined parameters. The CIF has been deposited at the Cambridge Crystallographic Data Centre, CCDC 1912548. Crystal data for **4**, $C_{36}H_{32}BN_3O_4{\cdot}{}^1/_2C_6H_{14}$, FW = 624.54, monoclinic space group $I2/a$, $a$ = 19.0173(9), $b$ = 18.1999(7), $c$ = 19.8837(9) Å, $\beta$ = 109.673(3)°, $T$ = 100 K, $Z$ = 8. A total of 171 402 data were collected with Mo K$\alpha$ radiation to $\theta_{max}$ = 35.0°, $R$ = 0.040 for 11,976 data with $I > 2\sigma(I)$ of 14,285 unique data ($R_{int}$ = 0.032), 429 refined parameters, CCDC 1912549; Crystal data for **5**, $C_{29}H_{28}BN_3O_4$, FW = 493.35, orthorhombic space group $P2_12_12_1$, $a$ = 7.0374(15), $b$ = 15.870(5), $c$ = 21.895(9) Å, $T$ = 90 K, $Z$ = 4. A total of 20 404 data were collected with Cu K$\alpha$ radiation to $\theta_{max}$ = 58.9°, $R$ = 0.093 for 1776 data with $I > 2\sigma(I)$ of 3509 unique data ($R_{int}$ = 0.336), 338 refined parameters, CCDC 1912550.

**Stability Study.** The stability of 25 mM solutions of BODIPYs **4** and **6** in $CDCl_3$ upon addition of 1 equiv of TFA was investigated by $^1H$ NMR and $^{11}B$ NMR spectra over a period of 24 h, at room temperature. The aqueous stability of 10 $\mu$M solutions of BODIPYs **2**−**5** in 1:1 DMSO/PBS at pH 7.4 and BODIPY **6** in 1:9 DMSO/PBS at pH 7.4 was investigated by UV−vis and fluorescence spectroscopies, up to 5 days at room temperature.

**Synthesis.** *General Procedure for the Preparation of BODIPY−Gly Derivatives **2**−**6**.* To a solution of BODIPY **1** (30 mg, 0.092 mmol) in 5 mL of dry dichloromethane under a nitrogen atmosphere was added $BCl_3$ (1 M in toluene, 0.22 mL, 0.185 mmol). The reaction was stirred for 1 h at room temperature, then 3 drops of dry triethylamine were added. The N-protected Gly (1−2 equiv) was dissolved in 2 mL of dry dichloromethane and 3 drops of dry triethylamine. The glycine solution was added dropwise to the $BCl_2$−BODIPY solution, and the final mixture was stirred at room temperature for 0.5 h. The reaction mixture was then poured into saturated aqueous $NaHCO_3$ and extracted with dichloromethane (10 mL × 3). The organic layers were combined and dried over anhydrous $Na_2SO_4$. The organic solvent was removed under reduced pressure and the residue was purified by column chromatography on silica gel, and then recrystallized to afford the desired BODIPYs **2**−**6**.

*Synthesis of BODIPY **2**.* BODIPY **2** was prepared from **1** (30.0 mg, 0.092 mmol) and *N*-(trifluoroacetyl)glycine (23.6 mg, 0.138 mmol, 1.5 equiv). The reaction mixture was purified using ethyl acetate/hexanes (1:2) for elution, yielding BODIPY **2** (10.5 mg, 0.023 mmol) in 25% yield, mp >140 °C (decomp). Two sets of peaks of isomers appear in NMR are referred as set A and set B in 1:0.3 ratio. $^1H$ NMR (400 MHz, $CDCl_3$): $\delta$ 7.55−7.30 (m, 6.5H, set A + set B), 6.04 (s, 2H, set A), 6.01 (s, 0.6H, set B), 4.40 (s, 0.6H, set B), 4.33 (s, 2H, set A), 2.28 (s, 1.8H, set B), 2.26 (s, 6H, set A), 1.40 (s, 6H, set A), 1.39 (s, 1.8H, set B). $^{13}C$ NMR (126 MHz, $CDCl_3$): $\delta$ 171.09, 155.32, 154.42, 145.22, 144.63, 142.87, 134.28, 132.65, 129.50, 129.42, 129.39, 129.24, 129.19, 128.07, 127.73, 127.66, 123.07, 122.90, 51.13, 14.76, 14.72, 14.66, 14.65; $^{11}B$ NMR (128 MHz, $CDCl_3$): $\delta$ 2.54 (s, set B), 1.83 (s, set A).$^{19}F$ NMR (471 MHz, $CDCl_3$) $\delta$ −73.35 (s, set A), −74.10 (s, set B). HRMS (ESI-TOF): $m/z$ $[M + H]^+$, 456.1693; calcd for $C_{23}H_{22}BF_3N_3O_3$, 456.1705.

*Synthesis of BODIPY **3**.* BODIPY **3** was prepared from **1** (30.0 mg, 0.092 mmol) and *N*-(*tert*-butoxycarbonyl)glycine (24.2 mg, 0.138 mmol, 1.5 equiv). The mixture was purified using dichloromethane/ethyl acetate/hexanes (1:1:2) for elution, yielding BODIPY **3** (15.0 mg, 0.033 mmol) in 36% yield, mp >170 °C (decomp). $^1H$ NMR (400 MHz, $CDCl_3$): $\delta$ 7.54−7.45 (m, 3H), 7.31−7.27 (m, 1H), 7.22−7.18 (m, 1H), 6.01 (s, 2H), 4.13 (s, 2H), 2.28 (s, 6H), 1.39 (s, 6H), 1.20 (s, 9H). $^{13}C$ NMR (126 MHz, $CDCl_3$): $\delta$ 173.77, 155.49, 155.15, 143.63, 142.06, 134.88, 132.76, 129.52, 129.20, 129.16, 128.20, 127.45, 122.46, 78.46, 49.90, 28.25, 14.68, 14.59. $^{11}B$ NMR (128 MHz, $CDCl_3$): $\delta$ 1.97 (s). HRMS (ESI-TOF): $m/z$ $[M + H]^+$, 460.2398; calcd for $C_{26}H_{31}BN_3O_4$, 460.2402.

*Synthesis of BODIPY **4**.* BODIPY **4** was prepared from **1** (30.0 mg, 0.092 mmol) and *N*-[(9*H*-fluoren-9-ylmethoxy)carbonyl]glycine (54.7 mg, 0.184 mmol, 2 equiv). The mixture was purified using ethyl acetate/hexanes (1:1) for elution, yielding BODIPY **4** (33.0 mg, 0.057 mmol) in 62% yield. mp >200 °C (decomp). Two sets of peaks of isomers appear in NMR are referred as set A and set B in 1:0.27 ratio. $^1H$ NMR (400 MHz, $CDCl_3$): $\delta$ 7.74−7.10 (m, 15.5H, set A + set B), 6.60 (d, $J$ = 7.6 Hz, 1H, set A), 6.10 (s, 2H, set A), 5.97 (s, 0.54H, set B), 4.44 (d, $J$ = 6.3 Hz, 0.54H, set B), 4.25 (s, 2H, set A), 4.17 (t, $J$ = 6.3 Hz, 0.27H, set B), 4.11 (d, $J$ = 7.3 Hz, 2H, set A), 4.02 (s, 0.54H, set B), 3.97 (t, $J$ = 7.3 Hz, 1H, set A), 2.36 (s, 6H, set A), 2.19 (s, 1.62H, set B), 1.37 (s, 1.62H, set B), 1,36 (s, 6H, set A). $^{13}C$ NMR (126 MHz, $CDCl_3$): $\delta$ 173.25, 156.15, 155.38, 144.27, 144.08, 142.67, 141.14, 134.44, 132.81, 125.05, 124.78, 122.75, 120.05, 119.88, 67.80, 50.45, 47.35, 14.90, 14.71. $^{11}B$ NMR (128 MHz, $CDCl_3$): $\delta$ 2.11 (s). HRMS (ESI-TOF): $m/z$ $[M + H]^+$, 582.2560; calcd for $C_{36}H_{33}BN_3O_4$, 582.2565

*Synthesis of Cbz BODIPY **5**.* BODIPY **5** was prepared from **1** (30.0 mg, 0.092 mmol) and *N*-(carbobenzyloxy)glycine (28.9 mg, 0.138 mmol, 1.5 equiv). The mixture was purified using ethyl acetate/hexanes (1:1) for elution, yielding BODIPY **5** (18.7 mg, 0.038 mmol) in 41% yield, mp >150 °C (decomp). Two sets of peaks of isomers appear in NMR are referred as set A and set B in 1:0.15 ratio. $^1H$ NMR (400 MHz, $CD_2Cl_2$): $\delta$ 7.43−7.18 (m, 8.5H, set A + set B), 6.89 (d, 2H, $J$ = 7.2 Hz, set A), 6.35 (d, 1H, $J$ = 7.6 Hz, set A), 6.03 (s, 0.3H, set B), 6.00 (s, 2H, set B), 5.01 (s, 0.3H, set B), 4.87 (s, 2H, set A), 4.12 (s, 2.3H, set A + set B), 2.26 (s, 6H, set A), 2.24 (s, 0.9H, set B), 1.40 (s, 0.9H, set B), 1.30 (s, 6H, set A). $^{11}B$ NMR (128 MHz, $CDCl_3$): $\delta$ 1.98 (s). $^{13}C$ NMR (126 MHz, $CDCl_3$): $\delta$ 173.47, 155.83, 155.04, 143.93, 142.49, 136.92, 134.52, 132.67, 129.10, 129.05, 128.98, 128.23, 127.70, 127.67, 127.58, 127.43, 66.45, 50.53, 14.79,



DOI: 10.1021/acs.inorgchem.9b01474
Inorg. Chem. 2019, 58, 11614−11621

14.56. HRMS (ESI-TOF): $m/z$ [M + H]$^+$, 494.2253; calcd for $C_{29}H_{29}BN_3O_4$, 494.2251

*Synthesis of BODIPY* **6**. BODIPY **6** was prepared from **1** (30.0 mg, 0.092 mmol) and *N*-acetylglycine (8.6 mg, 0.074 mmol, 0.8 equiv). The mixture was purified using ethyl acetate for elution, yielding BODIPY **6** (10.0 mg, 0.025 mmol) in 34% yield, mp >190 °C (decomp). $^1$H NMR (400 MHz, $CDCl_3$): $\delta$ 7.57−7.50 (m, 3H), 7.35−7.31 (m, 1H), 7.25−7.20 (m, 1H), 6.06 (s, 2H), 4.22 (s, 2H), 2.28 (s, 6H), 1.60 (s, 3H), 1.41 (s, 6H). $^{13}$C NMR (126 MHz, $CDCl_3$): $\delta$ 173.25, 171.57, 156.03, 144.85, 142.66, 134.21, 132.49, 129.53, 129.48, 129.42, 127.79, 127.65, 123.24, 50.00, 21.60, 14.82, 14.65. $^{11}$B NMR (128 MHz, $CDCl_3$): $\delta$ 2.18 (s). HRMS (ESI-TOF): $m/z$ [M + H]$^+$, 402.1990; calcd for $C_{23}H_{25}BN_3O_3$, 402.1988

## ■ ASSOCIATED CONTENT

### Supporting Information

The Supporting Information is available free of charge on the ACS Publications website at DOI: 10.1021/acs.inorgchem.9b01474.

$^1$H, $^{13}$C, $^{11}$B, and $^{19}$F NMR spectra, fluorescence and UV−vis spectra, stability study, and frontier orbitals for BODIPYs **1**−**6** (PDF)

### Accession Codes

CCDC 1912548−1912550 contain the supplementary crystallographic data for this paper. These data can be obtained free of charge via www.ccdc.cam.ac.uk/data_request/cif, or by emailing data_request@ccdc.cam.ac.uk, or by contacting The Cambridge Crystallographic Data Centre, 12 Union Road, Cambridge CB2 1EZ, UK; fax: +44 1223 336033.

## ■ AUTHOR INFORMATION


### Corresponding Author

*(M.G.H.V.) E-mail address: vicente@lsu.edu.

### ORCID

Petia Bobadova-Parvanova: 0000-0002-1965-419X

Frank R. Fronczek: 0000-0001-5544-2779

M. Graça H. Vicente: 0000-0002-4429-7868

### Author Contributions

‡These authors contributed equally.


### Notes

The authors declare no competing financial interest.

## ■ ACKNOWLEDGMENTS

This work was supported by the National Science Foundation (CHE-1800126). The authors are thankful to the Louisiana Optical Network Initiative (www.loni.org) for the use of their computer facilities.

## ■ REFERENCES


(1) Loudet, A.; Burgess, K. BODIPY Dyes and Their Derivatives: Syntheses and Spectroscopic Properties. *Chem. Rev.* **2007**, *107*, 4891−4932.

(2) Ziessel, R.; Ulrich, G.; Harriman, A. The Chemistry of Bodipy: A new El Dorado for Fluorescence Tools. *New J. Chem.* **2007**, *31*, 496−499.

(3) Ulrich, G.; Ziessel, R.; Harriman, A. The Chemistry of Fluorescent Bodipy Dyes: Versatility Unsurpassed. *Angew. Chem., Int. Ed.* **2008**, *47*, 1184−1201.

(4) Kolemen, S.; Akkaya, E. U. Reaction-Based BODIPY Probes for Selective Bio-Imaging. *Coord. Chem. Rev.* **2018**, *354*, 121−134.

(5) Kamkaew, A.; Lim, S. H.; Lee, H. B.; Kiew, L. V.; Chung, L. Y.; Burgess, K. BODIPY Dyes in Photodynamic Therapy. *Chem. Soc. Rev.* **2013**, *42*, 77−88.

(6) Boens, N.; Leen, V.; Dehaen, W. Fluorescent Indicators Based on BODIPY. *Chem. Soc. Rev.* **2012**, *41*, 1130−1172.

(7) Bessette, A.; Hanan, G. S. Design, Synthesis and Photophysical Studies of Dipyrromethene-Based Materials: Insights into Their Applications in Organic Photovoltaic Devices. *Chem. Soc. Rev.* **2014**, *43*, 3342−3405.

(8) Boens, N.; Verbelen, B.; Dehaen, W. Postfunctionalization of the BODIPY core: synthesis and spectroscopy. *Eur. J. Org. Chem.* **2015**, *2015*, 6577−6595.

(9) Buyukcakir, O.; Bozdemir, O. A.; Kolemen, S.; Erbas, S.; Akkaya, E. U. Tetrastyryl-Bodipy Dyes: Convenient Synthesis and Characterization of Elusive Near IR Fluorophores. *Org. Lett.* **2009**, *11*, 4644−4647.

(10) Yu, C.; Jiao, L.; Tan, X.; Wang, J.; Xu, Y.; Wu, Y.; Yang, G.; Wang, Z.; Hao, E. Straightforward Acid-Catalyzed Synthesis of Pyrrolyldipyrromethenes. *Angew. Chem., Int. Ed.* **2012**, *51*, 7688−7691.

(11) Xuan, S.; Zhao, N.; Ke, X.; Zhou, Z.; Fronczek, F. R.; Kadish, K. M.; Smith, K. M.; Vicente, M. G. H. Synthesis and Spectroscopic Investigation of A Series of Push−Pull Boron Dipyrromethenes (BODIPYs). *J. Org. Chem.* **2017**, *82*, 2545−2557.

(12) Zhao, N.; Xuan, S.; Zhou, Z.; Fronczek, F. R.; Smith, K. M.; Vicente, M. G. a. H. Synthesis and Spectroscopic and Cellular Properties of Near-IR [a] Phenanthrene-Fused 4, 4-Difluoro-4-bora-3a, 4a-diaza-s-indacenes. *J. Org. Chem.* **2017**, *82*, 9744−9750.

(13) Sheng, W.; Wu, Y.; Yu, C.; Bobadova-Parvanova, P.; Hao, E.; Jiao, L. Synthesis, Crystal Structure, and the Deep Near-Infrared Absorption/Emission of Bright AzaBODIPY-Based Organic Fluorophores. *Org. Lett.* **2018**, *20*, 2620−2623.

(14) Niu, S. L.; Ulrich, G.; Ziessel, R.; Kiss, A.; Renard, P.-Y.; Romieu, A. Water-Soluble BODIPY Derivatives. *Org. Lett.* **2009**, *11*, 2049−2052.

(15) Zhu, S.; Zhang, J.; Vegesna, G.; Luo, F.-T.; Green, S. A.; Liu, H. Highly Water-Soluble Neutral BODIPY Dyes with Controllable Fluorescence Quantum Yields. *Org. Lett.* **2011**, *13*, 438−441.

(16) Bura, T.; Ziessel, R. Water-Soluble Phosphonate-Substituted BODIPY Derivatives with Tunable Emission Channels. *Org. Lett.* **2011**, *13*, 3072−3075.

(17) Wang, M.; Vicente, M. G. H.; Mason, D.; Bobadova-Parvanova, P. Stability of a Series of BODIPYs in Acidic Conditions: An Experimental and Computational Study into the Role of the Substituents at Boron. *ACS Omega* **2018**, *3*, 5502−5510.

(18) Nguyen, A. L.; Wang, M.; Bobadova-Parvanova, P.; Do, Q.; Zhou, Z.; Fronczek, F. R.; Smith, K. M.; Vicente, M. G. H. Synthesis and Properties of B-Cyano-BODIPYs. *J. Porphyrins Phthalocyanines* **2016**, *20*, 1409−1419.

(19) Li, L.; Nguyen, B.; Burgess, K. Functionalization of the 4,4-Difluoro-4-bora-3a,4a-diaza-s-indacene (BODIPY) Core. *Bioorg. Med. Chem. Lett.* **2008**, *18*, 3112−3116.

(20) Bodio, E.; Goze, C. Investigation of BF Substitution on BODIPY and Aza-BODIPY Dyes: Development of B-O and B-C BODIPYs. *Dyes Pigm.* **2019**, *160*, 700−710.

(21) Wang, Z.; Cheng, C.; Kang, Z.; Miao, W.; Liu, Q.; Wang, H.; Hao, E. Organotrifluoroborate Salts as Complexation Reagents for Synthesizing BODIPY Dyes Containing Both Fluoride and an Organo Substituent at the Boron Center. *J. Org. Chem.* **2019**, *84*, 2732−2740.

(22) Lundrigan, T.; Crawford, S. M.; Cameron, T. S.; Thompson, A. Cl-BODIPYs: a BODIPY Class Enabling Facile B-Substitution. *Chem. Commun.* **2012**, *48*, 1003−1005.

(23) Lundrigan, T.; Thompson, A. Conversion of F-BODIPYs to Cl-BODIPYs: Enhancing the Reactivity of F-BODIPYs. *J. Org. Chem.* **2013**, *78*, 757−761.

(24) Ray, C.; Díaz-Casado, L.; Avellanal-Zaballa, E.; Bañuelos, J.; Cerdán, L.; García-Moreno, I.; Moreno, F.; Maroto, B. L.; López-Arbeloa, I.; de la Moya, S. N-BODIPYs Come into Play. Smart Dyes for Photonic Materials. *Chem. - Eur. J.* **2017**, *23*, 9383−9390.

(25) Zhang, G.; Wang, M.; Fronczek, F. R.; Smith, K. M.; Vicente, M. G. H. Lewis-Acid-Catalyzed BODIPY Boron Functionalization




DOI: 10.1021/acs.inorgchem.9b01474
*Inorg. Chem.* 2019, 58, 11614−11621

Using Trimethylsilyl Nucleophiles. *Inorg. Chem.* **2018**, *57*, 14493−14496.
(26) Rezende, L. C.; Emery, F. S. A Review of the Synthetic Strategies for the Development of BODIPY Dyes for Conjugation with Proteins. *Orbital: Electron. J. Chem.* **2013**, *5*, 62−83.
(27) Mendive-Tapia, L.; Zhao, C.; Akram, A. R.; Preciado, S.; Albericio, F.; Lee, M.; Serrels, A.; Kielland, N.; Read, N. D.; Lavilla, R.; Vendrell, M. Spacer-Free BODIPY Fluorogens in Antimicrobial Peptides for Direct Imaging of Fungal Infection in Human Tissue. *Nat. Commun.* **2016**, *7*, 10940.
(28) Wang, W.; Lorion, M. M.; Martinazzoli, O.; Ackermann, L. BODIPY Peptide Labeling by Late-Stage C(sp(3))-H Activation. *Angew. Chem., Int. Ed.* **2018**, *57*, 10554−10558.
(29) Stein, R. L. Mechanism of Enzymatic and Nonenzymatic Prolyl Cis-Trans Isomerization. *Adv. Protein Chem.* **1993**, *44*, 1−24.
(30) Cox, C.; Lectka, T. Synthetic Catalysis of Amide Isomerization. *Acc. Chem. Res.* **2000**, *33*, 849−858.
(31) Nguyen, A. L.; Bobadova-Parvanova, P.; Hopfinger, M.; Fronczek, F. R.; Smith, K. M.; Vicente, M. G. H. Synthesis and Reactivity of 4,4-Dialkoxy-BODIPYs: An Experimental and Computational Study. *Inorg. Chem.* **2015**, *54*, 3228−3236.
(32) Bobadova-Parvanova, P.; Galabov, B. Ab Initio Molecular-Orbital Study of Hydrogen-Bonded Complexes of Carbonyl Aliphatic Compounds and Hydrogen Fluoride. *J. Phys. Chem. A* **1998**, *102*, 1815−1819.
(33) Galabov, B.; Nikolova, V.; Ilieva, S. Does the Molecular Electrostatic Potential Reflect the Effects of Substituents in Aromatic Systems? *Chem. - Eur. J.* **2013**, *19*, 5149−5155.
(34) Nguyen, A. L.; Fronczek, F. R.; Vicente, M. G. H. CCDC 1912313: Experimental Crystal Structure Determination, 2019.
(35) Gibbs, J. H.; Robins, L. T.; Zhou, Z.; Bobadova-Parvanova, P.; Cottam, M.; McCandless, G. T.; Fronczek, F. R.; Vicente, M. G. H. Spectroscopic, Computational Modeling and Cytotoxicity of A Series of Meso-Phenyl and Meso-Thienyl-BODIPYs. *Bioorg. Med. Chem.* **2013**, *21*, 5770−5781.
(36) Kollmannsberger, M.; Gareis, T.; Heinl, S.; Daub, J.; Breu, J. Electrogenerated Chemiluminescence and Proton-Dependent Switching of Fluorescence: Functionalized Difluoroboradiaza-s-indacenes. *Angew. Chem., Int. Ed. Engl.* **1997**, *36*, 1333−1335.
(37) Kollmannsberger, M.; Rurack, K.; Resch-Genger, U.; Daub, J. Ultrafast Charge Transfer in Amino-Substituted Boron Dipyrromethene Dyes and Its Inhibition by Cation Complexation: A New Design Concept for Highly Sensitive Fluorescent Probes. *J. Phys. Chem. A* **1998**, *102*, 10211−10220.
(38) Tomasi, J.; Mennucci, B.; Cammi, R. Quantum Mechanical Continuum Solvation Models. *Chem. Rev.* **2005**, *105*, 2999−3094.
(39) Chai, J.-D.; Head-Gordon, M. Long-range corrected hybrid density functionals with damped atom-atom dispersion corrections. *Phys. Chem. Chem. Phys.* **2008**, *10*, 6615−20.
(40) Reed, A. E.; Weinstock, R. B.; Weinhold, F. Natural Population Analysis. *J. Chem. Phys.* **1985**, *83*, 735−746.
(41) Wolinski, K.; Hinton, J. F.; Pulay, P. Efficient Implementation of the Gauge-Independent Atomic Orbital Method for NMR Chemical Shift Calculations. *J. Am. Chem. Soc.* **1990**, *112*, 8251−8260.
(42) Woon, D. E.; Dunning, T. H. Gaussian Basis Sets for Use in Correlated Molecular Calculations. III. The Atoms Aluminum through Argon. *J. Chem. Phys.* **1993**, *98*, 1358.
(43) Lee, C.; Yang, W.; Parr, R. G. Development of the Colle-Salvetti Correlation-Energy Formula into a Functional of the Electron Density. *Phys. Rev. B: Condens. Matter Mater. Phys.* **1988**, *37*, 785.
(44) Lodewyk, M. W.; Siebert, M. R.; Tantillo, D. J. Computational Prediction of $^{1}$H and $^{13}$C Chemical Shifts: A Useful Tool for Natural Product, Mechanistic, and Synthetic Organic Chemistry. *Chem. Rev.* **2012**, *112*, 1839−1862.
(45) Bauernschmitt, R.; Ahlrichs, R. Treatment of Electronic Excitations within the Adiabatic Approximation of Time Dependent Density Functional Theory. *Chem. Phys. Lett.* **1996**, *256*, 454−464.
(46) Zhao, Y.; Truhlar, D. G. The M06 Suite of Density Functionals for Main Group Thermochemistry, Thermochemical Kinetics, Noncovalent Interactions, Excited States, and Transition Elements: Two New Functionals and Systematic Testing of Four M06-class Functionals and 12 other Functionals. *Theor. Chem. Acc.* **2008**, *120*, 215−241.
(47) Le Guennic, B.; Jacquemin, D. Taking up the Cyanine Challenge with Quantum Tools. *Acc. Chem. Res.* **2015**, *48*, 530−537.
(48) Frisch, M. J.; Trucks, G. W.; Schlegel, H. B.; Scuseria, G. E.; Robb, M. A.; Cheeseman, J. R.; Scalmani, G.; Barone, V.; Mennucci, B.; Petersson, G. A., et al. *Gaussian 09*, Revision D.01; Gaussian, Inc.: Wallingford, CT, 2009.


DOI: 10.1021/acs.inorgchem.9b01474
*Inorg. Chem.* 2019, 58, 11614−11621